Supplementary Material (ESI) for PCCP
This journal is © the Owner Societies 2011

EPR Parameters of Amino Acid Radicals in *P. eryngii* Versatile Peroxidase and its W164Y variant computed at the QM/MM level

Caterina Bernini,[a] *Rebecca Pogni,*[a] *Francisco J. Ruiz-Dueñas,*[b] *Angel T. Martínez,*[b]

Riccardo Basosi [a] *and Adalgisa Sinicropi* [a,*]

[a]*Department of Chemistry, University of Siena, 53100 Siena, Italy*
[b]*Centro de Investigaciones Biológicas, Consejo Superior de Investigaciones Cientificas, 28040 Madrid, Spain*

Supporting Information

Contents

1. Computational Details

1.1 Setup of the System

Initial structures for VP (pdb code: 2BOQ) and its W164Y variant (pdb code: 2W23) were obtained from the Protein Data Bank (1.33 Å and 1.94 Å resolution, respectively). The results of PROPKA2.0[1] runs were used, in combination with visual inspection, to assign the protonation states of all titratable residues (aspartic acid, glutamic acid and histidine) at the experimental pH (pH = 4.5). We assigned D30, D318, E26, E36, E40, E83, E140, E191, E217, E225 to be protonated, H39, H47, H232 to be protonated at the ε nitrogen and H169, which is coordinated to iron, to be protonated at the δ nitrogen. Missing hydrogen atoms were added by the psfgen module of VMD, version 1.8.6.[2] The protonated systems, as described above, with crystallographic water molecules, were neutralized with sodium and chlorine ions (0.15 M ionic strength) and fully solvated in a rectangular box (69 x 80 x 76 $Å^3$ for VP and 75 x 65 x 73 $Å^3$ for W164Y) of TIP3P water molecules using the autoionize and solvate modules of VMD.[2] Solvent boxes were created with a layer of at least 10 Å of water molecules around each protein atom and included 33975 and 31575 water molecules for VP and W164Y, respectively.

1.2 Force Field

All heme parameters were taken from the existing CHARMM27 library,[3] originally determined for a Fe^{2+} containing heme group,[4] with the exception that the atomic charges were modified to account for the different charge distribution in the Fe^{3+}-porphyrine complex.

Force Field atom types and charges for the heme used in the present work:

```
Atom
name
          type    charge
GROUP
ATOM FE   FE      1.68 !       O2A   O1A             O2D  O1D
ATOM NA   NPH    -0.76 !         \\ //                \\ //
ATOM NB   NPH    -0.76 !          CGA                  CGD
ATOM NC   NPH    -0.76 !           |                    |
ATOM ND   NPH    -0.76 !    HBA1--CBA--HBA2  HA   HBD1--CBD--HBD2
ATOM C1A  CPA     0.32 !           |          |          |
ATOM C2A  CPB    -0.03 !    HAA1--CAA-HAA2   _CHA_ HAD1--CAD--HAD2
ATOM C3A  CPB    -0.02 !           |       /     \       |
ATOM C4A  CPA     0.32 !          C2A---C1A       C4D---C3D
ATOM C1B  CPA     0.32 !           |     |         |     |
ATOM C2B  CPB    -0.02 !HMA1\      |     |         |     |      /HMD1
ATOM C3B  CPB    -0.03 !HMA2-CMA--C3A    NA       ND    C2D--CMD-HMD2
ATOM C4B  CPA     0.32 !HMA3/       \   / \       / \   /       \HMD3
ATOM C1C  CPA     0.32 !             C4A   \     /   C1D
ATOM C2C  CPB    -0.03 !            /       \   /       \
ATOM C3C  CPB    -0.02 !      HB--CHB        FE         CHD--HD
ATOM C4C  CPA     0.32 !            \       /   \       /
ATOM C1D  CPA     0.32 !             C1B   /     \   C4C        HAC
```

```
ATOM C2D  CPB    -0.02 !HMB1\       /   \ /       \ /   \       /
ATOM C3D  CPB    -0.03 !HMB2-CMB--C2B    NB       NC    C3C--CAC
ATOM C4D  CPA     0.32 !HMB3/      |     |         |     |     \\  /HBC1
GROUP                 !           |     |         |     |      CBC
ATOM CHA  CPM    -0.10 !          C3B---C4B       C1C---C2C        \HBC2
ATOM HA   HA      0.10 !           |       \_CHC_/       |
GROUP                 !          CAB         |         CMC--HMC3
ATOM CHB  CPM    -0.10 !         //  \        HC       /  |
ATOM HB   HA      0.10 !        CBB  HAB           HMC1  HMC2
GROUP                 !       /   \
ATOM CHC  CPM    -0.10 !    HBB1  HBB2
ATOM HC   HA      0.10 !
GROUP
ATOM CHD  CPM    -0.10
ATOM HD   HA      0.10
GROUP
ATOM CMA  CT3    -0.27
ATOM HMA1 HA      0.09
ATOM HMA2 HA      0.09
ATOM HMA3 HA      0.09
GROUP
ATOM CAA  CT2    -0.18
ATOM HAA1 HA      0.09
ATOM HAA2 HA      0.09
GROUP
ATOM CBA  CT2    -0.28
ATOM HBA1 HA      0.09
ATOM HBA2 HA      0.09
ATOM CGA  CC      0.62
ATOM O1A  OC     -0.76
ATOM O2A  OC     -0.76
GROUP
ATOM CMB  CT3    -0.27
ATOM HMB1 HA      0.09
ATOM HMB2 HA      0.09
ATOM HMB3 HA      0.09
GROUP
ATOM CAB  C      -0.20
ATOM HAB  HA      0.20
GROUP
ATOM CBB  C      -0.20
ATOM HBB1 HA      0.10
ATOM HBB2 HA      0.10
GROUP
ATOM CMC  CT3    -0.27
ATOM HMC1 HA      0.09
ATOM HMC2 HA      0.09
ATOM HMC3 HA      0.09
GROUP
ATOM CAC  C      -0.20
ATOM HAC  HA      0.20
GROUP
ATOM CBC  C      -0.20
ATOM HBC1 HA      0.10
ATOM HBC2 HA      0.10
GROUP
ATOM CMD  CT3    -0.27
ATOM HMD1 HA      0.09
ATOM HMD2 HA      0.09
ATOM HMD3 HA      0.09
GROUP
ATOM CAD  CT2    -0.18
ATOM HAD1 HA      0.09
```

```
ATOM HAD2 HA      0.09
GROUP
ATOM CBD  CT2    -0.28
ATOM HBD1 HA      0.09
ATOM HBD2 HA      0.09
ATOM CGD  CC      0.62
ATOM O1D  OC     -0.76
ATOM O2D  OC     -0.76
```

1.3 QM/MM Method

All QM/MM calculations were performed with the MOLCAS 7.4 package,[5] coupled with a modified version of the MM package Tinker 4.2.[6]
An electronic embedding scheme was applied, using hydrogen link atoms (HLA) with a scaled-charge model to treat the QM/MM boundary region.[7, 8]
The frontier is placed at the CO-CαH and NH–CαH bonds of V163 and L165, respectively, and at the Cα-Cβ bond of E243. The QM models **M1** and **M2** (see Scheme 1 of the main text) were employed in QM/MM calculations of VP and W164Y enzymes, respectively. Model **M1** (40 atoms) includes the tryptophan residue (W164) with the CO and NH bonds of V163 and L165, respectively, and the negatively charged glutamate residue (E243). Model **M2** (37 atoms) is comprised of the tyrosyl residue (Y164) with the CO and NH bonds of V163 and L165, respectively, and the glutamate residue (E243). In both cases the overall charge for the QM part is -1 for the non-radical species and 0 for the radical species.
To correctly describe the frontier the HLA may interact with all the MM point charges, but cannot be involved in other MM potentials. The charges of the frontier MM carbon atoms were set to 0 to ensure that the QM wavefunction is not overpolarized by the proximity of HLA atoms. This procedure is allowed by the small values of the original CHARMM27 point charges.

Table S1. Partial charges used for V163, L165 and E243 at the frontier region.

Residue	Charge					
	Cα	**Hα**	**N**	**H**	**C**	**O**
V163	0.0000	0.0000	-0.3740	0.3740	-	-
L165	0.0000	0.0000	-	-	0.5100	-0.5100
E243	0.0000	0.0000	-0.4284	0.3388	0.5548	-0.4652

Both subsystems (QM and MM) interact in the following way: (a) the QM wave function is polarized by all the MM point charges; (b) stretching, bending and torsion potentials involving at least one MM atom are described at the MM level; (c) standard van der Waals potentials are used to represent the interaction between atom pairs (QM/MM) separated by more than two bonds.
Therefore, the Hamiltonian used in the computations takes the following form:

$$\hat{H} = \hat{H}_{QM} + \hat{H}_{MM} + \sum_{i=1}^{n}\sum_{j=1}^{Q} -\frac{q_j}{r_{ij}} + \sum_{i=1}^{N}\sum_{j=1}^{Q}\frac{Z_i q_j}{r_{ij}} + E_{vdW} + E_{bonded}$$

where $\hat{H}_{QM}$ is the Hamiltonian of the QM subsystem *in vacuo*. $\hat{H}_{MM}$ is the Hamiltonian of the MM subsystem computed using the CHARMM27 forcefield, and the remaining four terms are the interacting QM/MM Hamiltonian. The first two terms comprise the electrostatic interactions (polarization of the wavefunction by the MM charges and Coulomb term between QM and MM nuclei) that were approximated using the ElectroStatic Potential Fitted method (ESPF) implemented in MOLCAS. The third term corresponds to the van der Waals interaction term computed using the definition of the CHARMM27 forcefield, and the last one contains the terms needed for a proper description of the frontier within the hydrogen link atom scheme. The active MM region has been defined to include all residues and solvent molecules that have atoms within a distance of 5 Å around any QM atoms and R257, K253 and S246 residues.
Here we explicitly specify the protein residues belonging to the chosen active region: P159, V160, E161, V162, V163, W164/Y164, L165, L166, A167, S168, F193, F198, Q239, T240, A241, E243, Q245, S246, M247, V248, N250, Q251, P252, K253, I254, Q255, N256, R257, F258, A259, A260, T261, M262.

2. Results

2.1 EPR magnetic parameters

The theoretical framework for present day EPR calculations is provided by hybrid DFT methods,[9-17] that give better results than those delivered by the "pure" functionals or by competing theories based on correlated *ab initio* methods.[18] Among hybrid functionals, B3LYP[19-21] gives good theoretical results for EPR spectroscopy. Viable alternatives are PBE0[9] and TPSSh.[22] For the calculations of EPR properties a predefined special basis set can be used, such as the polarized triple-ζ valence basis set TZVP or the Barone's[23, 24] EPR-II basis set. The spectroscopic data were obtained from additional single-point calculations at all sets of optimized structures using several hybrid density functionals (B3LYP, PBE0, TPSSh) in combination with the TZVP and EPR-II spectroscopic basis set for all atoms (see Table S2-16). These calculations were performed with the program package ORCA.[25]
For B3LYP/TZVP computed values and abbreviations see the main paper.

Table S2. g-tensors, hfcc (mT) and Mulliken spin densities computed for **VP_10ns-neu** structure.

		B3LYP/EPR-II	PBE0/EPR-II	PBE0/TZVP	TPSSh/EPR-II	TPSSh/TZVP
g-tensors						
g_i	**iso**	2.00280	2.00279	2.00285	2.00277	2.00283
	x	2.00341	2.00341	2.00350	2.00333	2.00343
	y	2.00268	2.00266	2.00274	2.00266	2.00274
	z	2.00231	2.00230	2.00232	2.00232	2.00233
hfcc						
A_i(H-β1)	**iso**	2.77	2.72	2.58	2.85	2.71
	x	2.65	2.60	2.45	2.74	2.60
	y	2.95	2.90	2.76	3.03	2.90
	z	2.71	2.66	2.51	2.79	2.65
A_i(H-β2)	**iso**	1.07	1.06	1.01	1.09	1.05
	x	1.02	1.00	0.95	1.03	0.93
	y	0.96	0.94	0.90	0.97	0.98
	z	1.24	1.23	1.19	1.26	1.22
A_i(H1)	**iso**	-0.08	-0.06	-0.06	-0.08	-0.06
	x	-0.23	-0.22	-0.22	-0.23	-0.21
	y	0.19	0.20	0.20	0.18	0.20
	z	-0.19	-0.17	-0.17	-0.18	-0.16
A_i(H2)	**iso**	-0.20	-0.19	-0.19	-0.24	-0.23
	x	-0.35	-0.34	-0.33	-0.38	-0.37
	y	0.06	0.07	0.07	0.02	0.03
	z	-0.32	-0.31	-0.30	-0.36	-0.34
A_i(H-5)	**iso**	-0.53	-0.51	-0.58	-0.58	-0.59
	x	-0.78	-0.75	-0.82	-0.83	-0.83
	y	-0.23	-0.22	-0.28	-0.27	-0.29
	z	-0.59	-0.57	-0.62	-0.64	-0.64
A_i(H-7)	**iso**	-0.44	-0.42	-0.47	-0.47	-0.47
	x	-0.15	-0.14	-0.19	-0.18	-0.19
	y	-0.69	-0.66	-0.73	-0.73	-0.72
	z	-0.47	-0.45	-0.50	-0.51	-0.51
A_i(N1)	**iso**	0.26	0.23	0.23	0.20	0.17
	x	-0.04	-0.08	-0.08	-0.10	-0.14
	y	-0.06	-0.09	-0.10	-0.12	-0.16
	z	0.89	0.88	0.87	0.83	0.80
spin densities						
N1		0.19	0.19	0.20	0.19	0.19
C2		0.03	0.01	-0.01	0.02	-0.02
C3		0.49	0.56	0.61	0.52	0.60
C5		0.22	0.26	0.28	0.23	0.27
C6		-0.07	-0.09	-0.12	-0.08	-0.11
C7		0.17	0.19	0.20	0.18	0.19
C8		0.02	0.01	0.01	0.02	0.03

Table S3. g-tensors, hfcc (mT) and Mulliken spin densities computed for **VP_9.8ns-neu** structure.

		B3LYP/EPR-II	PBE0/EPR-II	PBE0/TZVP	TPSSh/EPR-II	TPSSh/TZVP
g-tensors						
g_i	**iso**	2.00280	2.00279	2.00285	2.00277	2.00283
	x	2.00342	2.00342	2.00351	2.00333	2.00344
	y	2.00268	2.00265	2.00273	2.00266	2.00273
	z	2.00231	2.00230	2.00231	2.00232	2.00233
hfcc						
A_i(H-β1)	**iso**	2.77	2.72	2.58	2.85	2.71
	x	2.65	2.66	2.45	2.74	2.60
	y	2.95	2.90	2.77	3.03	2.90
	z	2.71	2.60	2.52	2.79	2.65
A_i(H-β2)	**iso**	1.01	1.00	0.96	1.02	0.98
	x	0.96	0.94	0.89	0.97	0.92
	y	0.90	0.88	0.84	0.91	0.87
	z	1.18	1.17	1.13	1.19	1.16
A_i(H1)	**iso**	-0.06	-0.06	-0.05	-0.06	-0.04
	x	-0.21	-0.20	-0.19	-0.20	-0.18
	y	0.19	0.19	0.20	0.17	0.19
	z	-0.17	-0.16	-0.15	-0.17	-0.14
A_i(H2)	**iso**	-0.21	-0.21	-0.20	-0.25	-0.23
	x	-0.35	-0.36	-0.34	-0.39	-0.38
	y	0.06	0.06	0.07	0.01	0.03
	z	-0.32	-0.32	-0.31	-0.36	-0.35
A_i(H-5)	**iso**	-0.53	-0.58	-0.57	-0.57	-0.58
	x	-0.76	-0.82	-0.81	-0.82	-0.82
	y	-0.23	-0.28	-0.28	-0.27	-0.29
	z	-0.58	-0.63	-0.61	-0.63	-0.63
A_i(H-7)	**iso**	-0.44	-0.49	-0.48	-0.48	-0.48
	x	-0.15	-0.19	-0.19	-0.18	-0.19
	y	-0.70	-0.76	-0.74	-0.74	-0.74
	z	-0.48	-0.52	-0.50	-0.52	-0.51
A_i(N1)	**iso**	0.27	0.26	0.23	0.21	0.17
	x	-0.04	-0.05	-0.08	-0.10	-0.14
	y	-0.05	-0.06	-0.10	-0.11	-0.15
	z	0.90	0.89	0.87	0.83	0.81
spin densities						
N1		0.19	0.19	0.20	0.19	0.19
C2		0.03	0.02	-0.01	0.02	-0.01
C3		0.49	0.53	0.61	0.52	0.60
C5		0.21	0.23	0.28	0.23	0.27
C6		-0.07	-0.09	-0.12	-0.08	-0.11
C7		0.17	0.19	0.21	0.18	0.20
C8		0.02	0.01	0.01	0.02	0.02

Table S4. g-tensors, hfcc (mT) and Mulliken spin densities computed for **VP_9.6ns-neu** structure.

		B3LYP/EPR-II	PBE0/EPR-II	PBE0/TZVP	TPSSh/EPR-II	TPSSh/TZVP
g-tensors						
g_i	**iso**	2.00279	2.00278	2.00285	2.00277	2.00284
	x	2.00341	2.00340	2.00352	2.00333	2.00346
	y	2.00266	2.00263	2.00272	2.00265	2.00273
	z	2.00231	2.00230	2.00231	2.00233	2.00233
hfcc						
A_i(H-β1)	**iso**	2.79	2.73	2.59	2.86	2.73
	x	2.67	2.61	2.47	2.75	2.61
	y	2.97	2.91	2.78	3.04	2.91
	z	2.73	2.67	2.53	2.80	2.66
A_i(H-β2)	**iso**	0.96	0.95	0.91	0.97	0.93
	x	0.91	0.90	0.85	0.92	0.87
	y	0.85	0.84	0.80	0.86	0.82
	z	1.13	1.12	1.08	1.14	1.10
A_i(H1)	**iso**	-0.09	-0.09	-0.07	-0.09	-0.07
	x	-0.25	-0.24	-0.23	-0.24	-0.22
	y	0.17	0.17	0.18	0.15	0.18
	z	-0.20	-0.19	-0.17	-0.19	-0.17
A_i(H2)	**iso**	-0.23	-0.24	-0.23	-0.27	-0.26
	x	-0.40	-0.40	-0.39	-0.43	-0.42
	y	0.05	0.04	0.05	0.01	0.01
	z	-0.35	-0.35	-0.34	-0.39	-0.38
A_i(H-5)	**iso**	-0.53	-0.58	-0.57	-0.58	-0.59
	x	-0.77	-0.83	-0.82	-0.83	-0.83
	y	-0.23	-0.28	-0.28	-0.27	-0.29
	z	-0.59	-0.63	-0.62	-0.64	-0.64
A_i(H-7)	**iso**	-0.43	-0.48	-0.46	-0.46	-0.46
	x	-0.15	-0.19	-0.18	-0.17	-0.18
	y	-0.68	-0.74	-0.72	-0.72	-0.71
	z	-0.46	-0.51	-0.49	-0.50	-0.50
A_i(N1)	**iso**	0.26	0.25	0.23	0.20	0.17
	x	-0.04	-0.05	-0.08	-0.10	-0.13
	y	-0.05	-0.06	-0.09	-0.11	-0.15
	z	0.88	0.87	0.85	0.81	0.79
spin densities						
N1		0.19	0.19	0.19	0.18	0.19
C2		0.04	0.03	0.01	0.03	0.00
C3		0.49	0.52	0.60	0.51	0.59
C5		0.21	0.23	0.28	0.23	0.27
C6		-0.07	-0.09	-0.12	-0.08	-0.10
C7		0.17	0.18	0.20	0.18	0.19
C8		0.02	0.01	0.01	0.02	0.03

Table S5. g-tensors, hfcc (mT) and Mulliken spin densities computed for **VP_9.4ns-neu** structure.

		B3LYP/EPR-II	PBE0/EPR-II	PBE0/TZVP	TPSSh/EPR-II	TPSSh/TZVP
g-tensors						
g_i	**iso**	2.00280	2.00279	2.00285	2.00276	2.00282
	x	2.00342	2.00342	2.00350	2.00332	2.00342
	y	2.00268	2.00266	2.00274	2.00266	2.00273
	z	2.00231	2.00230	2.00232	2.00231	2.00233
hfcc						
A_i(H-β1)	**iso**	2.78	2.73	2.59	2.87	2.73
	x	2.66	2.61	2.46	2.76	2.61
	y	2.96	2.91	2.78	3.05	2.92
	z	2.72	2.67	2.53	2.81	2.67
A_i(H-β2)	**iso**	1.03	1.01	0.97	1.04	1.00
	x	0.97	0.96	0.91	0.99	0.94
	y	0.92	0.90	0.86	0.93	0.89
	z	1.20	1.18	1.15	1.21	1.17
A_i(H1)	**iso**	-0.06	-0.06	-0.05	-0.06	-0.04
	x	-0.20	-0.20	-0.19	-0.20	-0.18
	y	0.18	0.19	0.20	0.17	0.19
	z	-0.16	-0.16	-0.15	-0.16	-0.14
A_i(H2)	**iso**	-0.18	-0.18	-0.17	-0.22	-0.21
	x	-0.32	-0.32	-0.31	-0.36	-0.34
	y	0.07	0.07	0.08	0.03	0.04
	z	-0.30	-0.30	-0.29	-0.34	-0.33
A_i(H-5)	**iso**	-0.53	-0.58	-0.57	-0.58	-0.59
	x	-0.78	-0.84	-0.82	-0.84	-0.84
	y	-0.23	-0.28	-0.28	-0.27	-0.29
	z	-0.59	-0.64	-0.62	-0.64	-0.64
A_i(H-7)	**iso**	-0.44	-0.48	-0.47	-0.47	-0.47
	x	-0.15	-0.19	-0.19	-0.18	-0.19
	y	-0.68	-0.74	-0.73	-0.73	-0.73
	z	-0.47	-0.51	-0.50	-0.51	-0.51
A_i(N1)	**iso**	0.28	0.27	0.24	0.21	0.18
	x	-0.04	-0.05	-0.10	-0.10	-0.14
	y	-0.05	-0.06	-0.08	-0.11	-0.16
	z	0.92	0.92	0.90	0.86	0.83
spin densities						
N1		0.20	0.20	0.20	0.20	0.20
C2		0.02	0.01	-0.02	0.01	-0.03
C3		0.50	0.53	0.61	0.52	0.60
C5		0.22	0.23	0.28	0.23	0.27
C6		-0.07	-0.09	-0.12	-0.08	-0.10
C7		0.17	0.18	0.20	0.18	0.19
C8		0.02	0.01	0.01	0.02	0.03

Table S6. g-tensors, hfcc (mT) and Mulliken spin densities computed for **VP_9.2ns-neu** structure.

		B3LYP/EPR-II	PBE0/EPR-II	PBE0/TZVP	TPSSh/EPR-II	TPSSh/TZVP
g-tensors						
g_i	**iso**	2.00280	2.00279	2.00285	2.00277	2.00283
	x	2.00342	2.00341	2.00349	2.00334	2.00344
	y	2.00267	2.00264	2.00272	2.00265	2.00272
	z	2.00231	2.00230	2.00232	2.00233	2.00234
hfcc						
A_i(H-β1)	**iso**	2.84	2.78	2.64	2.92	2.78
	x	2.72	2.66	2.51	2.81	2.66
	y	3.02	2.97	2.83	3.10	2.96
	z	2.78	2.73	2.58	2.86	2.71
A_i(H-β2)	**iso**	0.99	0.98	0.94	1.00	0.96
	x	0.94	0.92	0.88	0.95	0.90
	y	0.88	0.87	0.83	0.89	0.85
	z	1.16	1.15	1.12	1.17	1.14
A_i(H1)	**iso**	-0.07	-0.07	-0.06	-0.07	-0.05
	x	-0.22	-0.22	-0.21	-0.22	-0.20
	y	0.18	0.18	0.20	0.17	0.19
	z	-0.18	-0.17	-0.16	-0.18	-0.15
A_i(H2)	**iso**	-0.22	-0.22	-0.21	-0.26	-0.25
	x	-0.37	-0.37	-0.36	-0.41	-0.40
	y	0.06	0.05	0.06	0.01	0.02
	z	-0.33	-0.33	-0.32	-0.38	-0.36
A_i(H-5)	**iso**	-0.53	-0.58	-0.57	-0.57	-0.58
	x	-0.76	-0.83	-0.81	-0.82	-0.82
	y	-0.23	-0.28	-0.28	-0.27	-0.28
	z	-0.58	-0.63	-0.61	-0.63	-0.63
A_i(H-7)	**iso**	-0.45	-0.50	-0.48	-0.48	-0.49
	x	-0.15	-0.19	-0.19	-0.18	-0.19
	y	-0.70	-0.77	-0.75	-0.75	-0.74
	z	-0.48	-0.52	-0.51	-0.52	-0.52
A_i(N1)	**iso**	0.26	0.25	0.22	0.20	0.16
	x	-0.04	-0.05	-0.08	-0.10	-0.14
	y	-0.06	-0.07	-0.10	-0.12	0.16
	z	0.87	0.87	0.85	0.81	0.79
spin densities						
N1		0.19	0.19	0.19	0.19	0.19
C2		0.03	0.02	0.01	0.02	-0.01
C3		0.49	0.53	0.60	0.52	0.59
C5		0.21	0.23	0.28	0.23	0.27
C6		-0.07	-0.09	-0.12	-0.08	-0.11
C7		0.18	0.19	0.21	0.18	0.20
C8		0.01	-0.01	-0.01	0.01	0.02

Table S7. g-tensors, hfcc (mT) and Mulliken spin densities computed for **VP_10ns-cat** structure.

		B3LYP/EPR-II	PBE0/EPR-II	PBE0/TZVP	TPSSh/EPR-II	TPSSh/TZVP
g-tensors						
g_i	**iso**	2.00278	2.00275	2.00283	2.00283	2.00290
	x	2.00339	2.00337	2.00346	2.00338	2.00350
	y	2.00261	2.00256	2.00269	2.00271	2.00279
	z	2.00235	2.00233	2.00235	2.00239	2.00241
hfcc						
A_i(H-β1)	**iso**	2.49	2.45	2.32	2.54	2.42
	x	2.38	2.34	2.21	2.44	2.32
	y	2.65	2.62	2.50	2.70	2.59
	z	2.43	2.39	2.27	2.48	2.36
A_i(H-β2)	**iso**	0.94	0.93	0.89	0.94	0.91
	x	0.89	0.99	0.84	0.90	0.86
	y	0.83	0.82	0.79	0.83	0.80
	z	1.09	1.08	1.05	1.09	1.06
A_i(H1)	**iso**	-0.38	-0.37	-0.36	-0.36	-0.34
	x	-0.67	-0.67	-0.66	-0.65	-0.63
	y	0.06	0.06	0.07	0.06	0.07
	z	-0.51	-0.50	-0.49	-0.49	-0.47
A_i(H2)	**iso**	-0.35	-0.38	-0.36	-0.39	-0.38
	x	-0.46	-0.48	-0.46	-0.50	-0.48
	y	-0.01	-0.03	-0.02	-0.06	-0.05
	z	-0.58	-0.61	-0.59	-0.61	-0.59
A_i(H-5)	**iso**	-0.57	-0.62	-0.62	-0.62	-0.63
	x	-0.84	-0.91	-0.89	-0.90	-0.90
	y	-0.24	-0.29	-0.29	-0.28	-0.30
	z	-0.63	-0.68	-0.66	-0.68	-0.68
A_i(H-7)	**iso**	-0.46	-0.51	-0.49	-0.49	-0.49
	x	-0.15	-0.20	-0.19	-0.18	-0.19
	y	-0.72	-0.78	-0.76	-0.76	-0.75
	z	-0.50	-0.54	-0.52	-0.53	-0.53
A_i(N1)	**iso**	0.21	0.20	0.18	0.17	0.14
	x	-0.05	-0.06	-0.08	-0.09	-0.13
	y	-0.07	-0.07	-0.10	-0.11	-0.14
	z	0.75	0.74	0.73	0.70	0.68
spin densities						
N1		0.16	0.15	0.15	0.15	0.15
C2		0.10	0.10	0.08	0.09	0.06
C3		0.42	0.46	0.53	0.45	0.52
C5		0.23	0.25	0.29	0.24	0.29
C6		-0.08	-0.10	-0.12	-0.09	-0.11
C7		0.18	0.19	0.21	0.19	0.20
C8		0.04	0.03	0.04	0.05	0.06

Computed EPR parameters of tryptophan radicals were found almost independent of the choice of hybrid functional (B3LYP, PBE0 or TPSSh) and basis set (TZVP or EPR-II). Indeed, g-tensors and hfcc values computed for the same structure, using the six different combinations of functional and basis set displayed, vary within a maximum of 200 ppm and 0.2 mT, respectively.

Table S8. B3LYP/TZVP g-tensors, hfcc (mT) and Mulliken spin densities computed for **VP_10ns-TS**.

		g-tensors	hfcc							spin densities						
		g_i	A_i(H-β1)	A_i(H-β2)	A_i(H1)	A_i(H2)	A_i(H5)	A_i(H7)	A_i(N1)	N1	C2	C3	C5	C6	C7	C8
VP_10ns-TS	**iso**	2.00285	2.47	0.93	-0.25	-0.30	-0.54	-0.44	0.20	0.16	0.06	0.51	0.27	-0.10	0.20	0.04
	x	2.00348	2.35	0.87	-0.48	-0.41	-0.80	-0.15	-0.07							
	y	2.00273	2.65	0.82	0.12	0.01	-0.23	-0.71	-0.09							
	z	2.00234	2.41	1.09	-0.38	-0.50	-0.59	-0.48	0.77							

Table S9. B3LYP/TZVP g-tensors, hfcc (mT) and Mulliken spin densities computed for the QM/MM optimized geometry of a neutral tryptophan radical not H-bonded (**VP_10ns-neu-B**), obtained after breaking the N1-H1 hydrogen bond with E243 and allowing E243 residue to form a hydrogen bond with a nearby water molecule after rotation around the C-O2 bond.

		g-tensors	hfcc							spin densities						
		g_i	A_i(H-β1)	A_i(H-β2)	A_i(H1)	A_i(H2)	A_i(H5)	A_i(H7)	A_i(N1)	N1	C2	C3	C5	C6	C7	C8
VP_10ns-neu-B	**iso**	2.00296	2.85	1.02	0.00	-0.03	-0.47	-0.38	0.28	0.25	-0.08	0.61	0.24	-0.08	0.17	0.01
	x	2.00376	2.71	0.95	-0.02	-0.09	-0.67	-0.12	-0.11							
	y	2.00284	3.05	0.91	0.04	0.16	-0.21	-0.61	-0.12							
	z	2.00227	2.78	1.21	-0.01	-0.15	-0.52	-0.41	1.06							

Table S10. g-tensors, hfcc (mT) and Mulliken spin densities computed for **W164Y_10ns-B** structure.

		B3LYP/EPR-II	PBE0/EPR-II	PBE0/TZVP	TPSSh/EPR-II	TPSSh/TZVP
g-tensors						
g_i	**iso**	2.0052	2.0053	2.0053	2.0048	2.0049
	x	2.0087	2.0087	2.0090	2.0078	2.0079
	y	2.0047	2.0048	2.0047	2.0045	2.0045
	z	2.0023	2.0023	2.0023	2.0023	2.0023
hfcc						
A_i(H-β1)	**iso**	2.50	2.43	2.29	2.58	2.45
	x	2.63	2.57	2.43	2.72	2.59
	y	2.39	2.32	2.17	2.49	2.34
	z	2.46	2.40	2.26	2.55	2.41
A_i(H-β2)	**iso**	0.64	0.63	0.60	0.66	0.63
	x	0.58	0.57	0.54	0.60	0.57
	y	0.78	0.77	0.75	0.80	0.77
	z	0.56	0.55	0.53	0.57	0.55
A_i(H2)	**iso**	0.21	0.29	0.29	0.21	0.23
	x	0.19	0.24	0.25	0.18	0.20
	y	0.33	0.43	0.44	0.35	0.36
	z	0.11	0.18	0.18	0.11	0.13
A_i(H6)	**iso**	0.21	0.29	0.29	0.22	0.23
	x	0.20	0.25	0.26	0.19	0.21
	y	0.34	0.44	0.45	0.35	0.37
	z	0.11	0.18	0.18	0.12	0.12
A_i(H3)	**iso**	-0.63	-0.71	-0.69	-0.68	-0.68
	x	-0.94	-1.04	-1.02	-1.00	-0.99
	y	-0.24	-0.30	-0.30	-0.28	-0.29
	z	-0.71	-0.78	-0.76	-0.77	-0.76
A_i(H5)	**iso**	-0.65	-0.73	-0.71	-0.71	-0.72
	x	-0.96	-1.06	-1.04	-1.04	-1.03
	y	-0.25	-0.31	-0.31	-0.30	-0.32
	z	-0.74	-0.81	-0.79	-0.80	-0.80
spin densities						
C1		0.38	0.46	0.46	0.41	0.45
C2		-0.12	-0.15	-0.18	-0.14	-0.17
C3		0.25	0.31	0.31	0.27	0.30
C4		-0.01	-0.03	-0.05	-0.01	-0.03
C5		0.26	0.31	0.31	0.27	0.30
C6		-0.12	-0.15	-0.18	-0.14	-0.17
O1		0.35	0.36	0.36	0.35	0.35

Table S11. g-tensors, hfcc (mT) and Mulliken spin densities computed for **W164Y_9.8ns-B** structure.

		B3LYP/EPR-II	PBE0/EPR-II	PBE0/TZVP	TPSSh/EPR-II	TPSSh/TZVP
g-tensors						
g_i	**iso**	2.0051	2.0051	2.0052	2.0047	2.0048
	x	2.0083	2.0083	2.0086	2.0074	2.0076
	y	2.0047	2.0048	2.0047	2.0045	2.0045
	z	2.0023	2.0023	2.0023	2.0023	2.0023
hfcc						
A_i(H-β1)	**iso**	2.46	2.40	2.26	2.55	2.41
	x	2.60	2.54	2.40	2.68	2.55
	y	2.35	2.29	2.14	2.45	2.31
	z	2.43	2.37	2.23	2.52	2.38
A_i(H-β2)	**iso**	0.67	0.66	0.63	0.69	0.66
	x	0.61	0.60	0.57	0.63	0.60
	y	0.82	0.80	0.78	0.83	0.80
	z	0.59	0.58	0.55	0.60	0.58
A_i(H2)	**iso**	0.20	0.27	0.28	0.20	0.22
	x	0.18	0.23	0.24	0.18	0.19
	y	0.32	0.42	0.42	0.33	0.34
	z	0.10	0.17	0.17	0.10	0.11
A_i(H6)	**iso**	0.22	0.30	0.30	0.22	0.24
	x	0.20	0.25	0.26	0.19	0.21
	y	0.35	0.45	0.46	0.36	0.38
	z	0.12	0.19	0.19	0.12	0.13
A_i(H3)	**iso**	-0.61	-0.69	-0.67	-0.66	-0.66
	x	-0.91	-1.01	-0.99	-0.97	-0.96
	y	-0.23	-0.29	-0.28	-0.26	-0.27
	z	-0.69	-0.76	-0.74	-0.74	-0.74
A_i(H5)	**iso**	-0.66	-0.74	-0.72	-0.72	-0.72
	x	-0.97	-1.07	-1.05	-1.05	-1.04
	y	-0.25	-0.32	-0.31	-0.30	-0.32
	z	-0.74	-0.82	-0.80	-0.81	-0.81
spin densities						
C1		0.38	0.42	0.46	0.41	0.45
C2		-0.11	-0.14	-0.18	-0.13	-0.16
C3		0.25	0.27	0.30	0.26	0.29
C4		-0.01	-0.02	-0.05	-0.01	-0.03
C5		0.26	0.28	0.32	0.27	0.30
C6		-0.12	-0.16	-0.19	-0.14	-0.18
O1		0.35	0.36	0.36	0.34	0.35

Table S12. g-tensors, hfcc (mT) and Mulliken spin densities computed for **W164Y_9.6ns-B** structure.

		B3LYP/EPR-II	PBE0/EPR-II	PBE0/TZVP	TPSSh/EPR-II	TPSSh/TZVP
g-tensors						
g_i	**iso**	2.0051	2.0051	2.0052	2.0048	2.0048
	x	2.0085	2.0083	2.0086	2.0076	2.0078
	y	2.0047	2.0046	2.0047	2.0045	2.0044
	z	2.0023	2.0023	2.0023	2.0023	2.0023
hfcc						
A_i(H-β1)	**iso**	2.44	2.49	2.34	2.53	2.39
	x	2.58	2.63	2.49	2.66	2.53
	y	2.33	2.38	2.23	2.43	2.29
	z	2.41	2.47	2.32	2.49	2.36
A_i(H-β2)	**iso**	0.65	0.60	0.57	0.66	0.64
	x	0.59	0.53	0.50	0.60	0.57
	y	0.79	0.74	0.71	0.80	0.78
	z	0.57	0.52	0.49	0.58	0.56
A_i(H2)	**iso**	0.20	0.27	0.27	0.21	0.22
	x	0.18	0.23	0.24	0.18	0.20
	y	0.32	0.41	0.41	0.33	0.35
	z	0.10	0.17	0.16	0.11	0.11
A_i(H6)	**iso**	0.22	0.29	0.29	0.22	0.24
	x	0.20	0.25	0.25	0.19	0.21
	y	0.35	0.44	0.44	0.36	0.37
	z	0.12	0.17	0.17	0.12	0.13
A_i(H3)	**iso**	-0.62	-0.70	-0.68	-0.67	-0.67
	x	-0.92	-1.03	-1.00	-0.98	-0.98
	y	-0.23	-0.29	-0.28	-0.27	-0.28
	z	-0.70	-0.77	-0.75	-0.75	-0.74
A_i(H5)	**iso**	-0.66	-0.71	-0.69	-0.72	-0.73
	x	-0.98	-1.04	-1.01	-1.06	-1.05
	y	-0.25	-0.31	-0.30	-0.30	-0.32
	z	-0.74	-0.79	-0.77	-0.81	-0.81
spin densities						
C1		0.38	0.42	0.46	0.41	0.45
C2		-0.11	-0.15	-0.18	-0.13	-0.17
C3		0.25	0.28	0.30	0.26	0.29
C4		-0.01	-0.02	-0.05	-0.01	-0.03
C5		0.26	0.27	0.30	0.27	0.30
C6		-0.12	-0.16	-0.19	-0.14	-0.18
O1		0.34	0.35	0.36	0.34	0.35

Table S13. g-tensors, hfcc (mT) and Mulliken spin densities computed for **W164Y_9.4ns-B** structure.

		B3LYP/EPR-II	PBE0/EPR-II	PBE0/TZVP	TPSSh/EPR-II	TPSSh/TZVP
g-tensors						
g_i	**iso**	2.0053	2.0053	2.0054	2.0049	2.0049
	x	2.0088	2.0089	2.0091	2.0079	2.0080
	y	2.0047	2.0048	2.0047	2.0045	2.0044
	z	2.0023	2.0023	2.0023	2.0023	2.0023
hfcc						
A_i(H-β1)	**iso**	2.46	2.40	2.26	2.55	2.42
	x	2.60	2.53	2.40	2.68	2.55
	y	2.35	2.29	2.14	2.45	2.31
	z	2.43	2.37	2.23	2.52	2.38
A_i(H-β2)	**iso**	0.65	0.64	0.61	0.67	0.64
	x	0.59	0.58	0.55	0.61	0.58
	y	0.80	0.78	0.76	0.81	0.78
	z	0.57	0.56	0.54	0.58	0.56
A_i(H2)	**iso**	0.21	0.29	0.29	0.22	0.23
	x	0.19	0.24	0.25	0.19	0.21
	y	0.34	0.44	0.44	0.35	0.36
	z	0.11	0.19	0.18	0.12	0.13
A_i(H6)	**iso**	0.22	0.30	0.30	0.22	0.24
	x	0.20	0.25	0.26	0.19	0.21
	y	0.35	0.45	0.45	0.36	0.37
	z	0.11	0.19	0.18	0.12	0.13
A_i(H3)	**iso**	-0.64	-0.71	-0.69	-0.69	-0.69
	x	-0.95	-1.05	-1.02	-1.01	-1.00
	y	-0.24	-0.30	-0.30	-0.28	-0.29
	z	-0.72	-0.79	-0.76	-0.77	-0.76
A_i(H5)	**iso**	-0.65	-0.73	-0.71	-0.72	-0.72
	x	-0.96	-1.06	-1.04	-1.04	-1.03
	y	-0.26	-0.32	-0.31	-0.30	-0.32
	z	-0.74	-0.81	-0.78	-0.80	-0.80
spin densities						
C1		0.38	0.42	0.46	0.41	0.45
C2		-0.12	-0.15	-0.18	-0.14	-0.17
C3		0.26	0.28	0.31	0.27	0.30
C4		-0.01	-0.03	-0.06	-0.02	-0.04
C5		0.26	0.28	0.31	0.27	0.30
C6		-0.12	-0.16	-0.19	-0.14	-0.17
O1		0.35	0.36	0.37	0.35	0.35

Table S14. g-tensors, hfcc (mT) and Mulliken spin densities computed for **W164Y_9.2ns-B** structure.

		B3LYP/EPR-II	PBE0/EPR-II	PBE0/TZVP	TPSSh/EPR-II	TPSSh/TZVP
g-tensors						
g_i	**iso**	2.0050	2.0051	2.0052	2.0047	2.0048
	x	2.0083	2.0083	2.0086	2.0075	2.0076
	y	2.0046	2.0046	2.0047	2.0044	2.0044
	z	2.0023	2.0023	2.0023	2.0023	2.0023
hfcc						
A_i(H-β1)	**iso**	2.56	2.49	2.34	2.64	2.51
	x	2.70	2.63	2.49	2.78	2.65
	y	2.45	2.38	2.23	2.54	2.40
	z	2.53	2.47	2.32	2.61	2.47
A_i(H-β2)	**iso**	0.61	0.60	0.57	0.62	0.59
	x	0.55	0.53	0.50	0.56	0.53
	y	0.75	0.74	0.71	0.76	0.74
	z	0.53	0.52	0.49	0.53	0.51
A_i(H2)	**iso**	0.20	0.27	0.27	0.20	0.22
	x	0.18	0.23	0.24	0.18	0.20
	y	0.32	0.41	0.41	0.33	0.35
	z	0.09	0.17	0.16	0.10	0.11
A_i(H6)	**iso**	0.21	0.29	0.29	0.21	0.23
	x	0.19	0.25	0.25	0.19	0.21
	y	0.34	0.44	0.44	0.35	0.37
	z	0.10	0.17	0.17	0.11	0.12
A_i(H3)	**iso**	-0.62	-0.70	-0.68	-0.67	-0.67
	x	-0.93	-1.03	-1.00	-0.99	-0.99
	y	-0.23	-0.29	-0.28	-0.27	-0.28
	z	-0.70	-0.77	-0.75	-0.76	-0.75
A_i(H5)	**iso**	-0.63	-0.71	-0.69	-0.70	-0.70
	x	-0.94	-1.04	-1.01	-1.01	-1.01
	y	-0.24	-0.31	-0.30	-0.29	-0.31
	z	-0.72	-0.79	-0.91	-0.79	-0.78
spin densities						
C1		0.38	0.42	0.46	0.41	0.45
C2		-0.11	-0.15	-0.18	-0.13	-0.17
C3		0.25	0.28	0.30	0.27	0.29
C4		-0.01	-0.02	-0.04	-0.01	-0.03
C5		0.25	0.27	0.30	0.26	0.29
C6		-0.12	-0.15	-0.19	-0.14	-0.17
O1		0.34	0.35	0.36	0.34	0.35

Table S15. g-tensors, hfcc (mT) and Mulliken spin densities computed for **W164Y_10ns-A** structure.

		B3LYP/EPR-II	PBE0/EPR-II	PBE0/TZVP	TPSSh/EPR-II	TPSSh/TZVP
g-tensors						
g_i	**iso**	2.0044	2.0044	2.0045	2.0042	2.0043
	x	2.0064	2.0064	2.0067	2.0060	2.0062
	y	2.0045	2.0045	2.0046	2.0045	2.0045
	z	2.0023	2.0023	2.0023	2.0023	2.0023
hfcc						
A_i(H-β1)	**iso**	2.73	2.65	2.50	2.78	2.64
	x	2.87	2.80	2.65	2.92	2.79
	y	2.61	2.54	2.37	2.68	2.53
	z	2.69	2.62	2.46	2.75	2.60
A_i(H-β2)	**iso**	0.63	0.62	0.59	0.62	0.60
	x	0.57	0.55	0.52	0.56	0.54
	y	0.77	0.76	0.74	0.77	0.75
	z	0.54	0.53	0.51	0.54	0.52
A_i(H2)	**iso**	0.16	0.23	0.23	0.16	0.18
	x	0.14	0.20	0.20	0.14	0.15
	y	0.28	0.36	0.37	0.29	0.30
	z	0.06	0.12	0.12	0.06	0.07
A_i(H6)	**iso**	0.17	0.24	0.25	0.17	0.19
	x	0.16	0.21	0.22	0.15	0.17
	y	0.29	0.38	0.39	0.30	0.32
	z	0.07	0.14	0.14	0.07	0.08
A_i(H3)	**iso**	-0.54	-0.61	-0.59	-0.58	-0.58
	x	-0.81	-0.90	-0.88	-0.86	-0.85
	y	-0.18	-0.23	-0.23	-0.22	-0.23
	z	-0.63	-0.69	-0.67	-0.67	-0.66
A_i(H5)	**iso**	-0.61	-0.69	-0.67	-0.68	-0.68
	x	-0.92	-1.01	-0.99	-1.00	-0.99
	y	-0.22	-0.28	-0.27	-0.27	-0.29
	z	-0.70	-0.77	-0.75	-0.77	-0.77
spin densities						
C1		0.39	0.43	0.46	0.42	0.45
C2		-0.09	-0.13	-0.15	-0.11	-0.14
C3		0.21	0.23	0.25	0.22	0.24
C4		0.04	0.03	0.02	0.04	0.03
C5		0.24	0.26	0.29	0.25	0.28
C6		-0.10	-0.14	-0.17	-0.12	-0.16
O1		0.31	0.32	0.32	0.31	0.31

The B3LYP and PBE0 EPR parameters, computed for the same structures of tyrosyl radicals, resulted to vary more than in the case of tryptophan radicals (e.g., g-tensors range within 300 ppm). The TPSSh functional provided computed g_x values about 1000 ppm lower than those computed using the other functionals. In any case, hfcc values computed for tyrosyl radicals vary within 0.3 mT.

Table S16. B3LYP/TZVP g-tensors, hfcc (mT) and Mulliken spin densities computed for a QM/MM optimized structure of tyrosyl radical (**W164Y_10ns-B2**) obtained from the optimized **W164Y_10ns-B** model, following a subsequent QM/MM optimization in which R257 side chain were included in the QM region (see also Table S18).

	g-tensors	hfcc						spin densities						
	g_i	A_i(H-β1)	A_i(H-β2)	A_i(H2)	A_i(H6)	A_i(H3)	A_i(H5)	C1	C2	C3	C4	C5	C6	O1
iso	2.0053	2.29	0.62	0.21	0.21	-0.61	-0.62	0.42	-0.15	0.28	-0.03	0.28	-0.15	0.36
x	2.0089	2.44	0.55	0.20	0.20	-0.92	-0.92							
y	2.0047	2.18	0.76	0.33	0.33	-0.23	-0.23							
z	2.0023	2.26	0.54	0.10	0.10	-0.69	-0.70							

Computed EPR parameters for **W164Y_10ns-B** and **W164Y_10ns-B2** models are very similar (see Table 4 in the main paper). Accordingly, the comparison of geometrical parameters shown in the following Table S18 with data in Table 6 of the main paper for the **W164Y_10ns-B** model indicates that the inclusion of R257 side chain in the QM region, which has a high computational cost, does not affect the QM/MM optimized geometry. In particular, the distance between the O1 tyrosyl oxygen and the hydrogen of the closest -NH_2 group of R257 is almost invariant between the two structures.

2.2 Optimized Structures

Table S17. Selected geometrical parameters[a] for B3LYP/CHARMM optimized geometries of VP neutral tryptophan radical.

System	ϕ	N1-H1	N1-C2	N1-C9	C2-C3	C3-C4	C4-C5	C4-C9	C5-C6	C6-C7	C7-C8	C8-C9	H1-O2	θ_1[b]	θ_2[b]	ρ_{C3}[b]
VP_9.8ns-neu	-22.960	1.531	1.322	1.420	1.456	1.427	1.406	1.422	1.398	1.397	1.414	1.382	1.071	-7.1	-52.9	0.53
VP_9.6ns-neu	-23.831	1.501	1.323	1.419	1.454	1.426	1.405	1.419	1.399	1.395	1.413	1.380	1.084	-6.0	-54.0	0.53
VP_9.4ns-neu	-23.035	1.547	1.322	1.420	1.455	1.429	1.407	1.423	1.400	1.397	1.415	1.382	1.066	-7.3	-52.7	0.53
VP_9.2ns-neu	-23.740	1.514	1.318	1.419	1.452	1.426	1.406	1.424	1.400	1.397	1.415	1.382	1.066	-6.2	-53.8	0.54
VP_10ns-neu-B	-25.950	4.049	1.317	1.419	1.448	1.432	1.399	1.425	1.402	1.396	1.414	1.383	0.994	-6.5	-53.3	0.58

[a]Distances in Å; angles in degrees. [b]Dihedral angles θ_1 and θ_2 and spin density ρ_{C3} are obtained by solving the McConnell relationships, using the program developed by Svistunenko (freely available at the URL http://privatewww.essex.ac.uk/~svist/) and providing the B3LYP/TZVP computed A_{iso}(H-β1) and A_{iso}(H-β2) values (B"=5.0 mT).

Table S18. Selected geometrical parameters[a] for the B3LYP/CHARMM optimized geometry of tyrosyl radical in **W164Y_10ns-B2** model.

System	ϕ	O1-C4	O1-H1	H1-O2	C1-C2	C1-C6	C2-C3	C3-C4	C4-C5	C5-C6	O1--H(NH)[b]	O1--H(OH)[c]	θ_1[d]	θ_2[d]	ρ_{C1}[d]
W164Y_10ns-B2	-29.522	1.259	3.094	0.971	1.419	1.419	1.373	1.456	1.450	1.368	2.008	4.542	-1.3	-58.7	0.40

[a]Distances in Å; angles in degrees. [b]Distance between O1 tyrosyl oxygen and the hydrogen of the closest -NH_2 group of R257. [c]H-bond distance between tyrosine O1 and the nearest water molecule. [d]Dihedral angles θ_1 and θ_2 and spin density ρ_{C1} are obtained by solving the McConnell relationships, using the program developed by Svistunenko (freely available at the URL http://privatewww.essex.ac.uk/~svist/) and providing the B3LYP/TZVP computed A_{iso}(H-β1) and A_{iso}(H-β2) values (B"=5.8 mT).

2.3 QM/MM Energies

Table S19. Absolute energies (Hartree) for DFT/CHARMM optimized structures of VP tryptophan radical (see Fig. 1).

System	B3LYP/6-31G**#	B3LYP/cc-pVTZ//B3LYP/6-31G**#	CASPT2/6-31G*//B3LYP/6-31G**#
VP_10ns-cat	-1051.30788	-1051.64834	-1048.05816
VP_10ns-TS	-1051.30425	-1051.64282	-1048.05306
VP_10ns-neu	-1051.31282	-1051.64958	-1048.06198

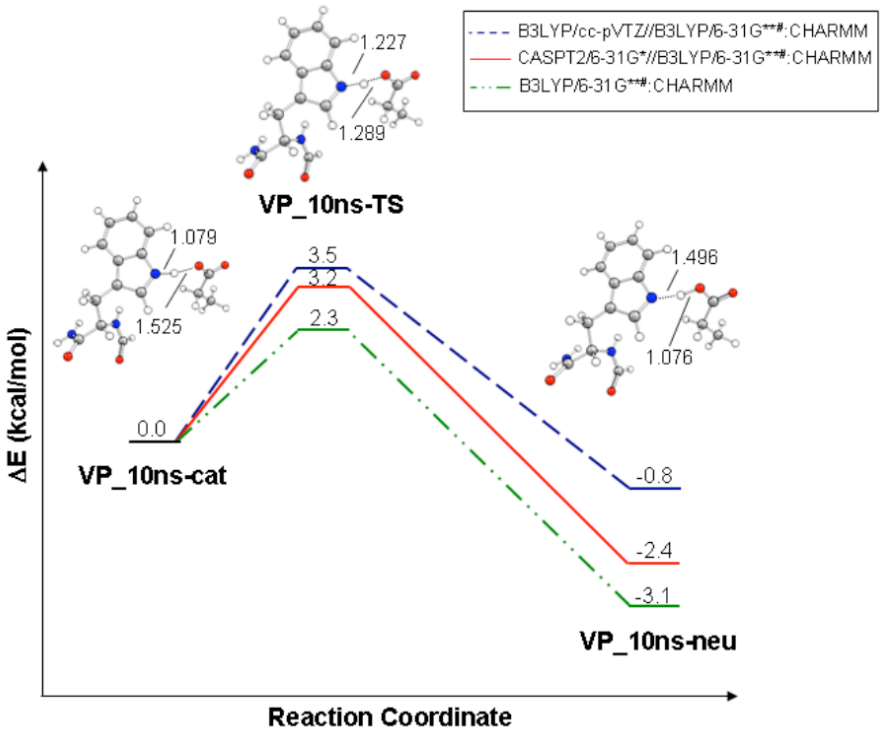

Figure S1. QM/MM energy profiles for the proton transfer in **VP_10ns** model. The relative energies (kcal/mol) of tryptophan radical cation (**VP_10ns-cat**), transition state (**VP_10ns-TS**) and neutral tryptophan radical (**VP_10ns-neu**) were computed at the B3LYP/6-31G**#:CHARMM optimized structures using different levels of theory (see inset). The N1-H1 and H1-O2 bond lengths are given in Å.

3. References

1 H. Li, A. D. Robertson, J. H. Jensen, *Proteins* 2005, **61**, 704.
2 W. Humphrey, A. Dalke, K. Schulten, *J. Molec. Graphics* 1996, **14.1**, 33.
3 A. D. MacKerell Jr., D. Bashford, M. Bellott, R. L. Dunbrack Jr., J. D. Evanseck, M. J. Field, S. Fischer, J. Gao, H. Guo, S. Ha, D. Joseph-McCarthy, L. Kuchnir, K. Kuczera, F. T. K. Lau, C. Mattos, S. Michnick, T. Ngo, D. T. Nguyen, B. Prodhom, W. E. Reiher III, B. Roux, M. Schlenkrich, J. C. Smith, R. Stote, J. Straub, M. Watanabe, J. Wiórkiewicz-Kuczera, D. Yin, M. Karplus, *J. Phys. Chem. B* 1998, **102**, 3586.
4 K. Kuczera, J. Kuriyan, M. Karplus, *J. Mol. Biol.* 1990, **213**, 351.
5 G. Karlström, R. Lindh, P.-A. Malmqvist, B. O. Roos, U. Ryde, V. Veryazov, P.-O. Widmark, M. Cossi, B. Schimmelpfennig, P. Neogrady, L. Seijo, *Comput. Mat. Sci.* 2003, **28**, 222.
6 J. W. Ponder 2004, Tinker4.2 - software tools for molecular design, Available at: http://dasher.wustl.edu/tinker
7 T. Andruniow, N. Ferré, M. Olivucci, *Proceed. Nat. Acad. Sci.* 2004, **101**, 17908–17913.
8 N. Ferré, M. Olivucci, *THEOCHEM* 2003, **632**, 71–82.
9 V. Barone, P. Cimino, *J. Chem. Theor. Comput.* 2009, **5**, 192.
10 D. A. Svistunenko, G. A. Jones, *Phys. Chem. Chem. Phys.* 2009, **11**, 6600.
11 B. Brogioni, D. Biglino, A. Sinicropi, E. Reijerse, P. Giardina, G. Sannia, W. Lubitz, R. Basosi, P. R., *Phys. Chem. Chem. Phys.* 2008, **10**, 7284.
12 M. Pavone, P. Cimino, O. Crescenzi, A. Sillanpää, V. Barone, *J. Phys. Chem. B* 2007, **111**, 8928.
13 M. van Gastel, W. Lubitz, G. Lassmann, F. Neese, *J. Am. Chem. Soc.* 2004, **126**, 2237.
14 S. Sinnecker, M. Flores, W. Lubitz, *Phys. Chem. Chem. Phys.* 2006, **8**, 5659.
15 D. Baute, D. Arieli, F. Neese, H. Zimmermann, B. M. Weckhuysen, D. Goldfarb, *J. Am. Chem. Soc.* 2004, **126**, 11733.
16 S. Un, *Magn. Res. Chem.* 2005, **43**, S229.
17 F. Neese, *J. Biol. Inorg. Chem.* 2006, **11**, 702–711.
18 F. Neese, T. Petrenko, D. Ganyushin, G. Olbrich, *Coord. Chem. Rev.* 2007, **251**, 288.
19 A. D. Becke, *J. Chem. Phys.* 1993, **98**, 5648.
20 C. Lee, W. Yang, R. G. Parr, *Phys. Rev. B* 1988, **37**, 785–789.
21 P. J. Stephens, F. J. Devlin, C. F. Chabalowski, M. J. Frisch, *J. Phys. Chem.* 1994, **98**, 11623.
22 F. Neese, *EPR Newsletter* 2009, **18**, 4.
23 V. Barone, Recent Advances in Density Functional Methods (PartI), ed. D.P. Chong ed., World Scientific Publishing Co., 1995.
24 V. Barone, A. Polimeno, *Phys. Chem. Chem. Phys.* 2006, **8**, 4609–4629.
25 F. Neese, ORCA, an ab initio, Density Functional and Semi-empirical Program Package, University of Bonn, Germany, Version 2.7, June 2009
26 B. O. Roos, in Adv. Chem. Phys. (Ab initio Methods in Quantum Chemistry-II), Vol. 69 (Ed.: K. P. Lawley), Wiley, New York, 1987, p. 399.
27 K. Andersson, P.-Å. Malmqvist, B. O. Roos, *J. Chem. Phys.* 1992, **96**, 1218– 1226.